

Capacitor-within-Capacitor: Electrically Controlled Elements

H. Grebel

Electronic Imaging Center, NJIT, University Heights, Newark, NJ 07102. grebel@njit.edu

Abstract: Capacitors are typically connected together in one of two configurations: either in series, or in parallel. Here, a new capacitive element is introduced: a capacitor-within-capacitor (CWC). The overall capacitance of the new structure is larger than an ordinary two-plate capacitor by at least 50% and its capacitance may be electrically controlled. When the 'ordinary' dielectric layers between plates were replaced by tissues soaked with ionic liquid, an increase of ca 10,000 was observed. Overall, this concept is deemed suitable for large capacity energy storage and tunable electronic circuitry.

I. Introduction:

Energy storage elements are an inherent part of modern electrical grids. They are used as secondary energy sources and are an integral part of sustainable sources, such as solar panels. The most prevalent energy storage, the battery, is slow to charge and discharge. Instead, it was suggested that quickly charged capacitors and in particular, supercapacitors should be used instead [1-5]. While supercapacitors may deliver large currents in a relatively short time frame, their overall energy storage is rather limited in comparison with ordinary batteries. Hence, there is a dire need to increase the energy storage of supercapacitors. Most of the efforts to date have been invested in materials rather than in new structural designs. Here, simulations are provided for a new capacitive structure: in addition to the obvious cathode (positive) and anode (negative) nodes, a third element – the gate – is introduced between them.

Energy storage elements are essential to a new family of micro-grids where delivery of energy is made in energy packets (the "digital grid") [6]. Such systems are expected to save at least 15% of energy and allow direct energy transfer, e.g., from a user with solar panels to another user in need of energy. The role of an energy storage system, which momentarily captures the energy and quickly releases it, thus becomes very important. It is expected that energy storage elements will not only serve as back-up energy sources but will also smooth power fluctuations in traditional electric grids. For example, spikes produced when turning motors on can bring down the entire micro-grid.

Supercapacitors are electrolytic capacitors whose increased capacitance is the result of a Helmholtz double layer at the electrolyte/metal interface (Fig. 1a). Specifically, the capacitance of a typical parallel plate capacitor is given by: $C=\epsilon A/d$. Here ϵ is the effective permittivity of the cell's electrolyte, A is the area of each electrode and, d , is the effective charge separation length. Most efforts to date were devoted to optimizing the anode, cathode and the electrolyte materials. Instead, let us concentrate on modifying the separator layer to be electrically active [7, Fig. 1b]. Such an approach was used in the past for corrosion protection [8-10] and could be implemented for supercapacitors, where a third, permeable electrode (the gate electrode) was placed between the anode and the cathode [11-14]. Since the average energy, stored within a capacitor is, $U=(1/2)CV^2$, where V is the potential difference between the plates, the question is whether the capacitance of an ordinary capacitor and perhaps a supercapacitor can be further increased by simply redesigning its structure.

In equivalent circuit terms, capacitors may be connected in series (the overall capacitance becomes smaller than either capacitor), or in parallel (the overall capacitance is the sum of the individual capacitors). Here we consider a third possibility, a capacitor-within-capacitor (CWC).

Two possible configurations are simulated below. The first configuration is more beneficial to dielectric capacitors. The other is more beneficial to supercapacitors and takes into account the double-layer formed near each electrodes. Experimental data are provided in further support of this concept.

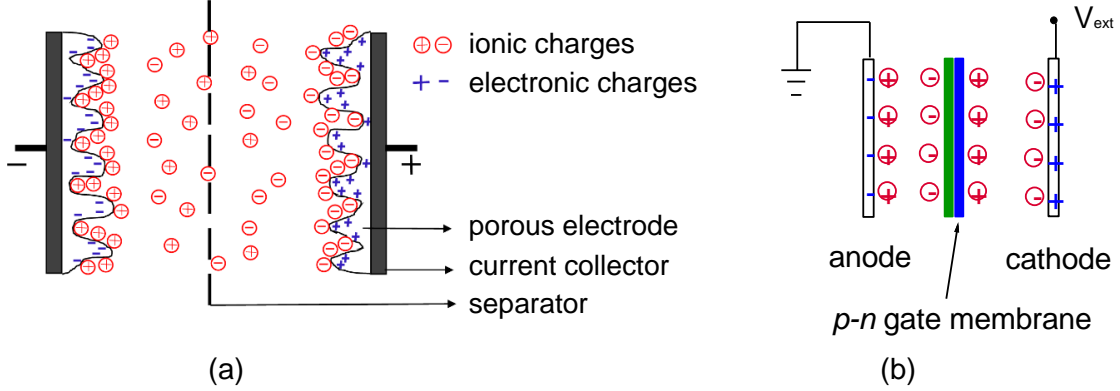


Fig. 1 (a) Basics of supercapacitors. (b) Structured supercapacitor: the separator becomes electrically active. Here, green – p-type; blue – n-type; both are porous films.

II. Simulations:

Dielectric capacitor: A dielectric capacitor is shown in Fig. 2. The outer capacitor (C_{cell}) is polarized when a potential V_0 is biasing the cell's electrodes. The controlling inner capacitor (the gate capacitor) may be polarized by biasing it with V_{gate} . A finite-element code (Comsol) was used for simulations. The cell's capacitance is simply the calculated terminal charge divided by the cell's voltage ($V_0=1$ V in our case). The structure was assumed to be immersed in a liquid dielectric with a relative dielectric constant of $\epsilon_r=100$.

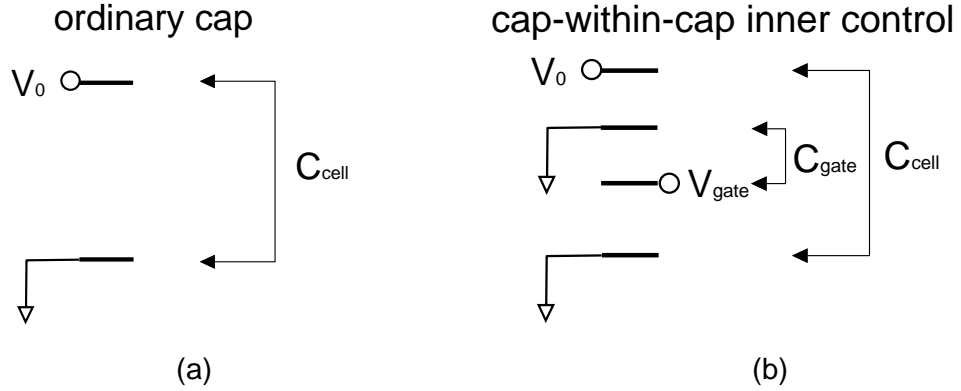


Fig. 2. (a) An ordinary dielectric capacitor. (b) A structure made of a capacitor-within-capacitor: the inner capacitor is polarized such that its polarization negates the polarization of the cell. A reverse structure, where the cell is defined by the inner plates and control is made by the outer plates is described in the SI Section.

The potential distribution for an ordinary and structured dielectric capacitor is shown in Fig. 3. An ordinary capacitor exhibits a linear electric potential distribution across its structure (Fig. 3a) and constant capacitance as a function of V_{gate} (Fig. 3c). If one includes an inner capacitor (Fig. 3b), then the electrical potential distribution changes and the overall cell's capacitance varies as a function of the gate voltage. The overall cell's capacitance has increased by a factor of ca 3.

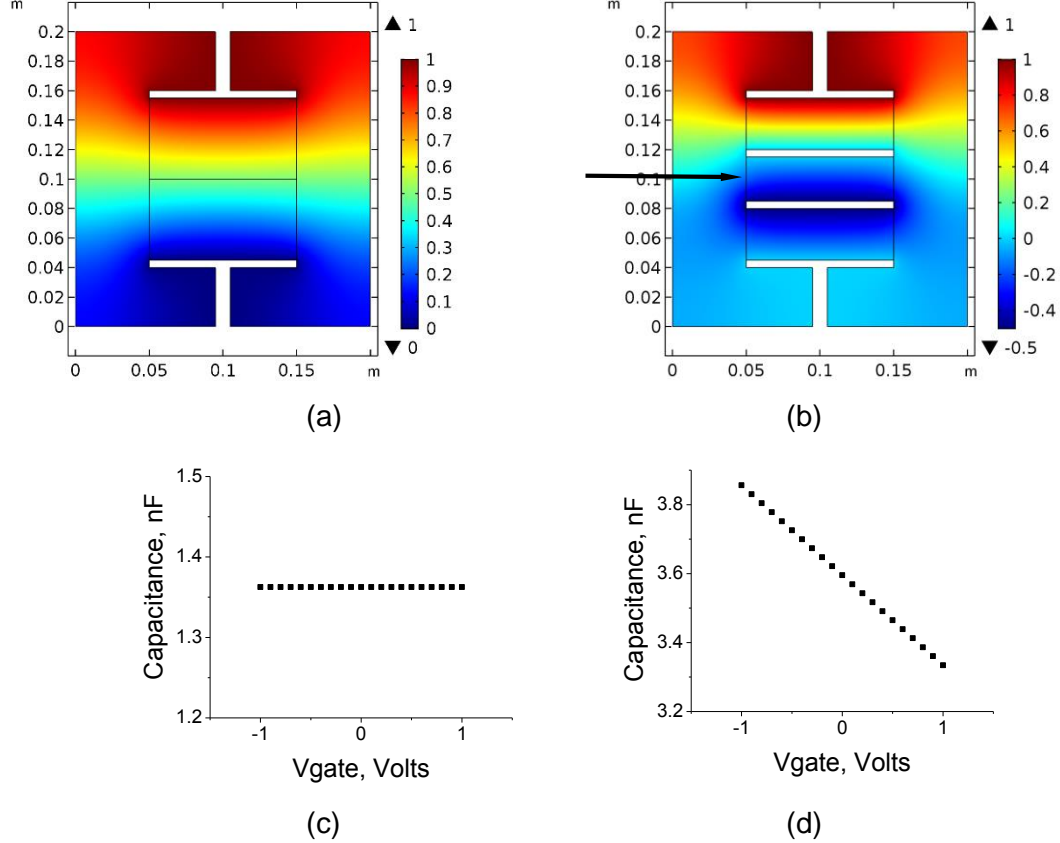


Fig. 3. (a) Ordinary capacitor: electric potential distribution when $V_0=1$ V. (b) Electric potential distribution when an inner capacitor, the gate capacitor is added. Shown is the distribution for $V_{\text{gate}}=-0.5$ V. The gate bias was provided to the bottom of the gate structure (see Fig. 2b) while its top electrode was grounded. The arrow points to the gate capacitor. (c) Without the inner gate capacitor, the capacitance (charge per unit cell's voltage) as a function of the gate voltage is obviously constant. (d) The capacitance is linearly varying as a function of V_{gate} .

Supercapacitors: In supercapacitors, a capacitance layer (the Helmholtz double layer) is formed at each metal/electrolyte interface. Each interface was modelled as a separate capacitor and connected to the other elements by line resistors as shown in Fig. 4. The line resistors represent the electrolyte; yet ideally the electrolytic resistance is very small and can be considered zero. The gate capacitor is made of three capacitors: one for each metal/electrolyte interface and one for the gate capacitor itself. Further structures may be made by replacing the inner gate capacitor with a junction or a potential barrier. For now, analysis is provided for only Fig. 4a.

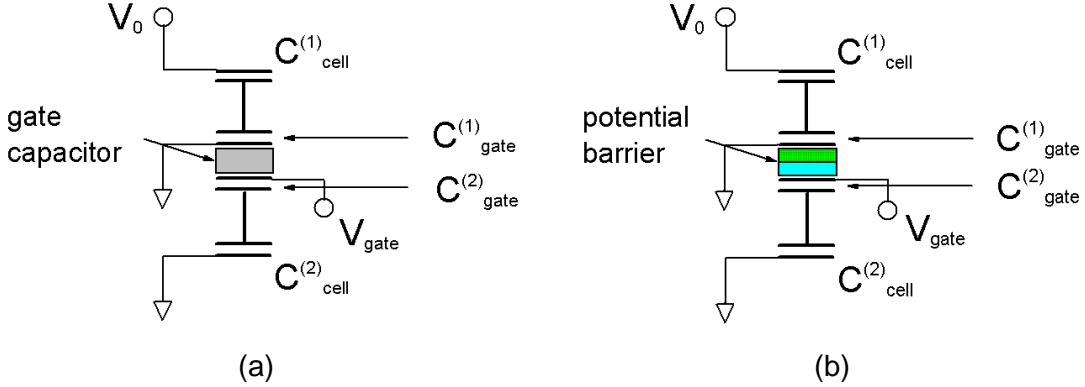
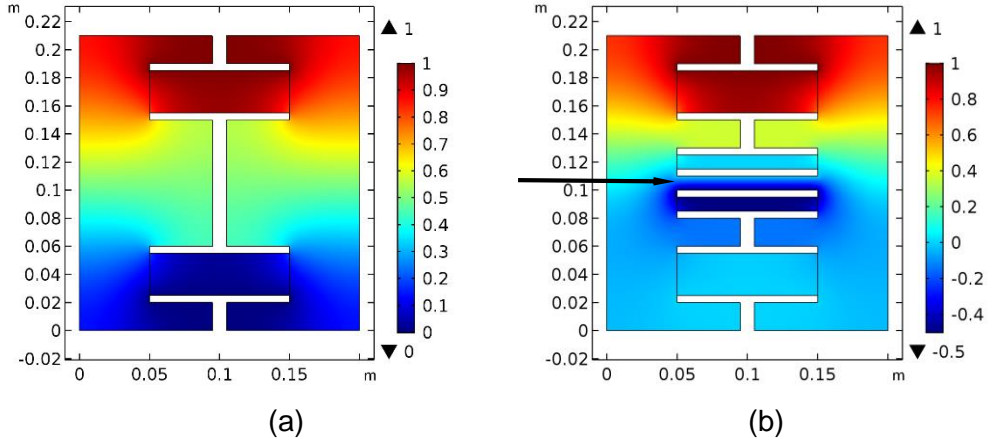


Fig. 4. A model where each interface forms a double layer capacitor. The $C^{(1)}_{\text{cell}}$, $C^{(2)}_{\text{cell}}$ are the capacitors of the upper and lower cell's interfaces, respectively. The corresponding interfaces for the gate electrodes are $C^{(1)}_{\text{gate}}$, $C^{(2)}_{\text{gate}}$, respectively. The two interfacial gate capacitors are part of the gate capacitor, which is formed between them (a), or, there might be an addition potential barrier, such as a porous diode, that separates them (b).

Results for configuration depicted in Fig 4a are shown in Fig. 5. Again the structured capacitor exhibits a larger cell's capacitance compared with an un-structured case; here, the structured configuration exhibits a capacitance increase of ca 2. The variation of the cell's capacitance as a function of V_{gate} is larger compared with the previous case; by almost 100%.



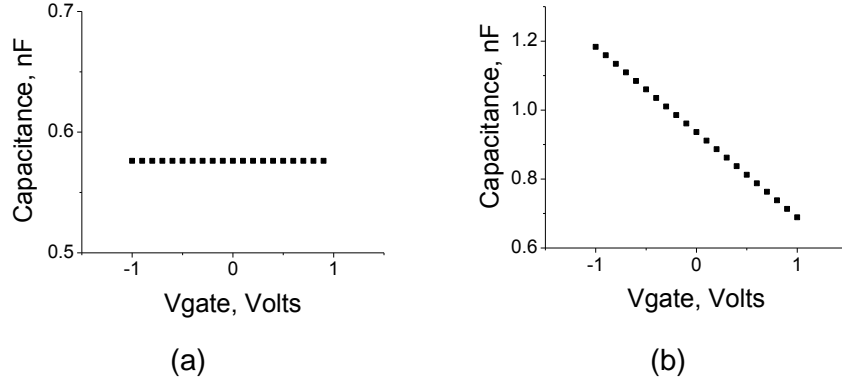


Fig. 5. Each metal/electrolyte interface is modeled by a capacitor. The electrolyte is modeled by a small resistor. (a) Ordinary supercapacitor: electric potential distribution when $V_0=1$ V. (b) Electric potential distribution when an inner capacitor, the gate capacitor is added. Shown is the distribution for $V_{gate}=-0.5$ V. The gate bias was provided to the bottom of the gate structure (see Fig. 2b) while its top electrode was grounded. The arrow points to the gate capacitor. (c) Without the inner gate capacitor, the capacitance (charge per unit cell's voltage) is obviously constant. (d) The capacitance is linearly varying as a function of V_{gate} .

III. Measurements:

Methodology: the $4 \times 4 \text{ cm}^2$ electrodes were made out of 25 micron copper foil, with a protruding notch in each plate, left for contact. This way, the thickness of the electrode has not been altered by a wire contact. The dielectric material was a 110 micron thick plastic transparency film and the entire structure was held between two glass plates by two paper clips. A 90 micron soaked lens tissue with ionic liquid (1-n-Butyl-3-methylimidazolium hexafluorophosphate) served as an electrolyte for super-capacitor like measurements. A hand held multi-meter (BK Precision) and LCR bridge (QuadTech) were used for the capacitance measurements. The simulations were DC calculations whereas a typical capacitance measurement employs a small AC signal. Under small AC signal approximation any independent DC voltage source is treated as a short due to the small internal battery impedance. Indeed, the measured cell capacitance, with a gate battery in place, was exactly the same as for the case where the two gate plates were short. In order to observe the effect of the gate bias on the cell capacitance at AC frequencies, one needs to synchronize it with the cell's measurements or dope the dielectric layers.

For the AC measurements, an external trigger (not shown) drove the scope and Ground was provided by the function-generator. Since the system may have its own capacitance, a reference trace of only the signal is provided below (Fig. 9). The system capacitance is smaller than the cell's capacitance when including the open gate structure (Fig. 10).

(a) Control of the capacitance by inner set of electrodes:

The configuration is depicted in Fig. 6a. Results obtained with a hand-held unit are shown in Fig. 6b-c.

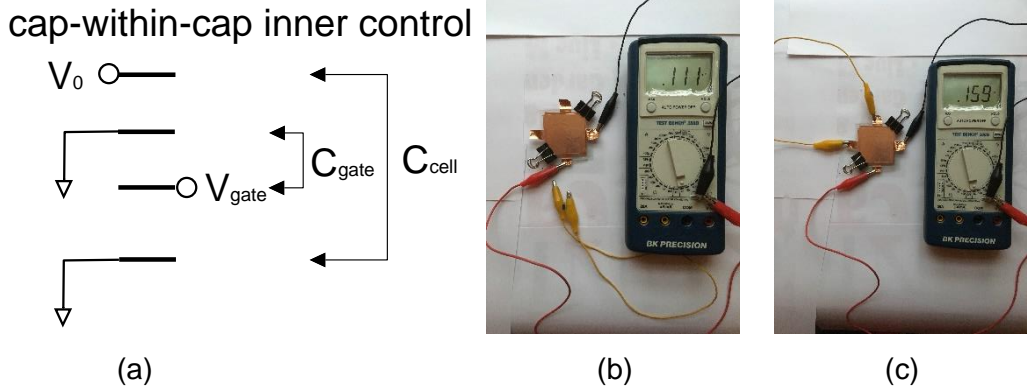


Fig. 6. (a) The configuration (from Fig. 2b). (b) Experiment: the inner gate electrodes were open the capacitance was 0.11 nF. (c) Experiment: the inner gate electrodes were short (connected by a yellow jumper). The capacitance was 0.16 nF. Red wire: positive cell's contact; black wire: negative cell's contact; the yellow jumper provides contact between the inner (gate) electrodes.

(b) Reverse Design: control of the capacitance by outer set of electrodes:

A reverse design and its simulation are provided in Figs 7. Experimental results are shown in Fig. 8. Note a factor of ~ 2 when comparing data shown in Figs 3d and Fig. 8a.

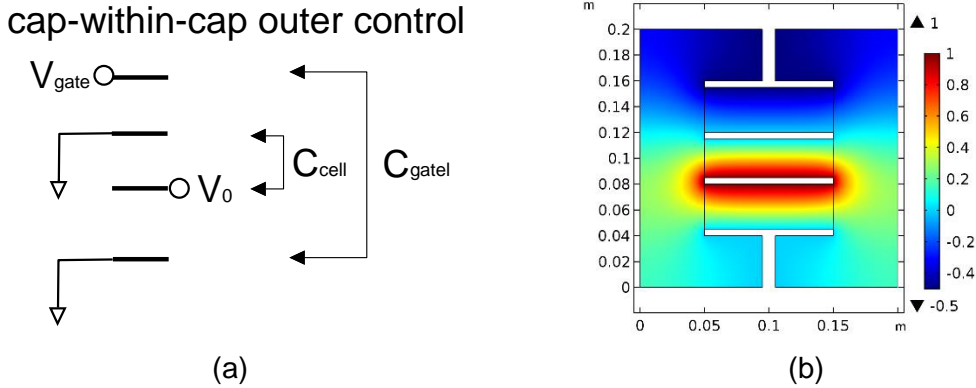


Fig. 7. (a) Reversing the roles of capacitor-within-capacitor: the controlled capacitance is measured for the inner electrodes whereas the controlling gate capacitor is provided by the outer electrode set. (b) Potential distribution when the outer electrodes are biased at $V_g = -0.5$ V.

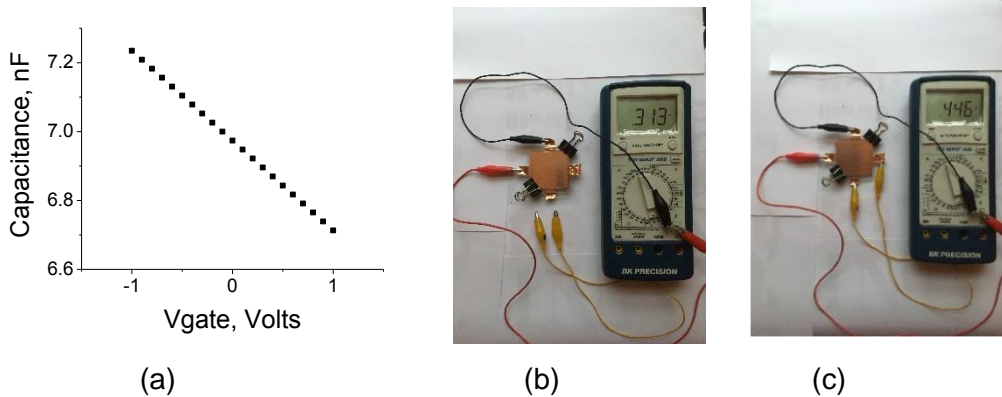


Fig. 8. (a) Simulations for Fig. 7. (b) Experiment: the outer gate electrodes were open. The capacitance was 0.31 nF due to 3 times smaller electrode separation of Fig 6a. (c) Experiment: the outer gate electrodes were short (connected by a yellow jumper). The capacitance was 0.45 nF. Red wire: positive cell's contact; black wire: negative cell's contact; the yellow jumper provides contact between the outer (gate) electrodes.

Capacitance as a function of the gate's shunt resistance is provided in Fig. 9. As the resistance varies, so is the capacitance of the cell.

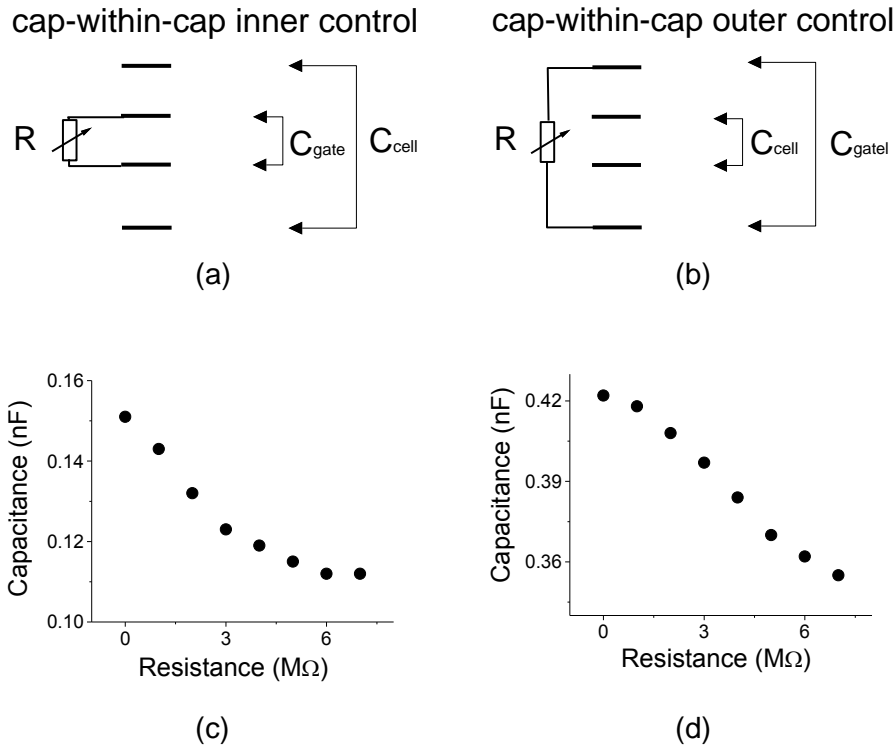


Fig. 9. The experimental configuration for an inner control (a) and an outer control (b). (c) Cell's capacitance as a function of resistance; inner gate control. (d) Cell's capacitance as a function of resistance; outer gate control. $C=0.29$ nF when the gate cap was open. The capacitor has been disassembled and put together before each set of experiments.

For the super-capacitor, we replaced the 'ordinary' plastic dielectric with an ionic liquid; a 90 micron thick lens tissue was soaked with the liquid for 30 minutes. The results are summarized in Table 1. Note the factor of ca 10,000 when the ionic liquid replaced the 'ordinary' dielectric.

Gate Control	Gate Status	Cell's Capacitance (μF)
inner	open	23.6
inner	short	34.5
outer	open	66.4
outer	short	93.2

Table 1: Electrolytic CWC with ionic liquid

(c) AC measurements:

The overall capacitance of the cell may be accessed through the rise, or decay time of a 10 KHz square wave. The signal was applied to the outer terminals (Figs. 10, 11a1-a2) using a function-generator. A $1\text{ K}\Omega$ resistor was connected in series between the function-generator and the positive outer terminal leads. A reference experiment is described in Fig. 10b. For the gated experiments, the same square wave was used as a gating signal, and was applied to the inner capacitor. Results are shown in Fig. 11b). If the polarity of the gate counters the polarity of the cell capacitor (Fig. 11a2), then, the time constant and hence the overall cell's capacitance increases (Fig. 11b2). If the polarity of the gate capacitor is in same the direction as the cell's polarity, then, the overall cell's capacitance decreases (Fig. 11b3).

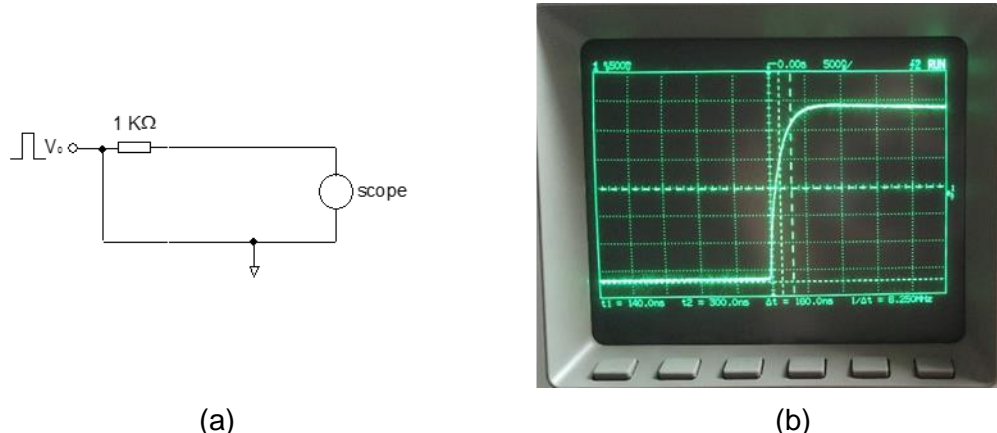


Fig. 10. Reference data. (a) The circuit. (b) Rise-time of a square wave without the structured capacitor indicates some system capacitance. Dielectric spacers were used.

Open and biased cases are shown in Fig. 11. They demonstrate how one may increase (or decrease) the overall cell's capacitance by re-structuring the CWC.

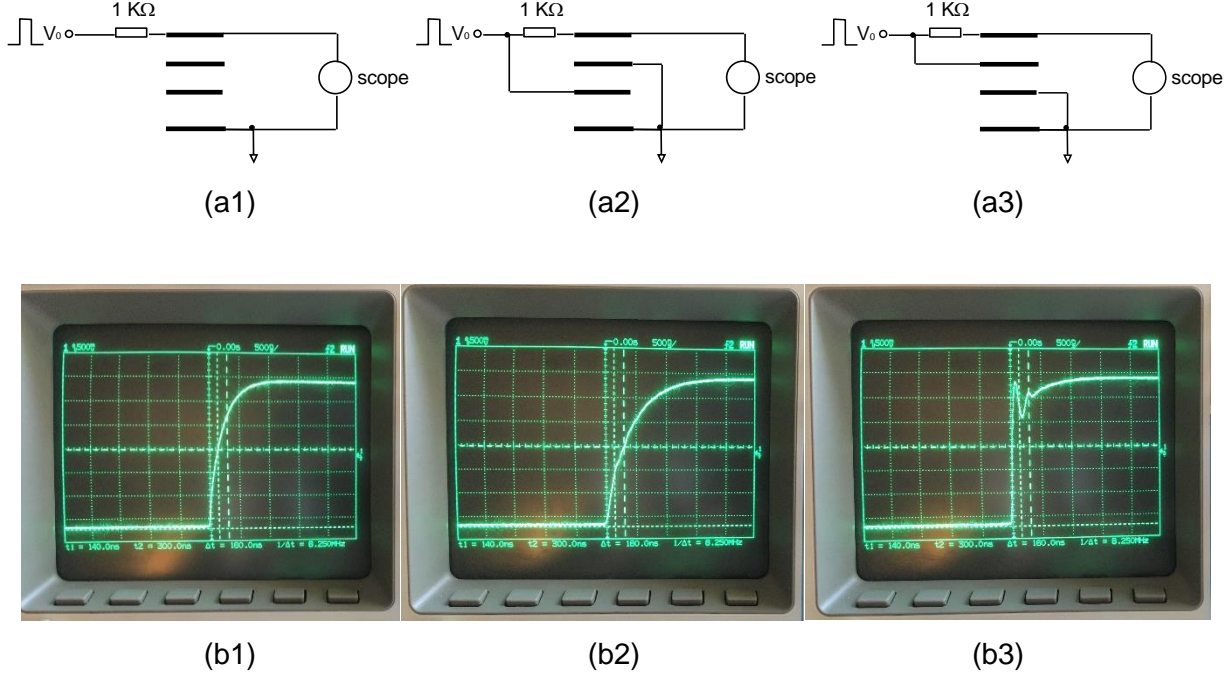


Fig 11. (a1)-(a3) The circuits. (b1-b3) Traces of Voltage vs Time. (b1) The (inner) gate capacitor was open; (b2) the polarity of the (inner) gate capacitor was opposite to the polarity of the (outer) cell capacitor and the rise time-constant increased; (b3) the polarity of the (inner) gate capacitor was in the direction of the cell's polarity and the rise time-constant decreased.

III. Discussion:

One may naively expect that the overall cell's capacitance should be reduced due to capacitors that are seemingly connected in series. This is not the case here because the capacitors are incorporated within an outer capacitor (the capacitor-within-capacitor concept). The increase in capacitance of the cell suggests some sort of capacitors connected in parallel. Rather, the polarity of the gate capacitor dictates the polarity of the electrolyte filling the cell (the dielectric constant, so to speak). The larger this polarity is, the larger would be the cell's capacitance. Such induced capacitance is similar to conditional artificial dielectrics [15]; which in itself is an extension to the concept of artificial dielectrics – dielectrics that are filled with metallic objects to affect their permittivity values [16]. Another point of view is as follows: the gate capacitor draws counter charges to its electrodes resulting in more electronic charges drawn to the cell's electrodes. The cell's capacitance C , the terminal charge Q and the cell's voltage V_0 are related through, $Q=CV_0$. Since the cell's voltage $V=V_0$ is kept constant, variations in the terminal charge would affect the overall cell's capacitance, C . We note that charging the gate capacitor costs energy through charge displacement but may exhibit little dissipating power losses; after charging, the gate current becomes zero.

The particularities of the inner (gate) capacitor only marginally affect the overall cell's capacitance. Specifically, varying the permittivity of the gate membrane by three orders of magnitudes, from 1 to 10^3 changes the overall cell's capacitance by less than 1%. That means that the larger effect is related to the induced surface charges across the inner structure.

Simulations for a reverse design (the cell capacitor is defined by the inner set of electrodes and the control (gate) capacitor were provided. The actual spacing between the inner electrode's set remained the same, namely, three times smaller than the spacing between the (outer) cell electrodes of Fig. 2b. As a result, the overall cell's capacitance was three times larger. Upon connecting the two outer gate electrodes with a wire, the overall capacitance has further increased by 30% compared with its open gate structure. When replacing the dielectric layer with ionic liquid, an increase of ca 50% was observed for the inner and outer gate control with an overall capacitance increase of ca 10,000 with respect to the case with a plastic dielectric film.

IV. Conclusions:

In summary, adding a biased capacitive element within (super)capacitors substantially increases the overall cell's capacitance. Such design suggests ultra-high supercapacitors for energy storage applications. Such capacitive structure is very suitable for programmable charging and discharging sequences through electronic control. By varying its capacitance, one may achieve a better impedance matching when integrating a supercapacitor with a rechargeable battery.

References:

1. John R. Miller and Patrice Simon, Electrochemical Capacitors for Energy Management, *Science*, 321 (2008), 651-652.
2. Zhong-Shuai Wu, Guangmin Zhou, Li-Chang Yin, Wencai Ren, Feng Li and Hui-Ming Cheng, Graphene/metal oxide composite electrode materials for energy storage, *Nano Energy*, 1 (2012) 107-131.
3. R. Kötz, and M. Carlen, Principles and applications of electrochemical capacitors – ScienceDirect, *Electrochimica Acta*, 45 (2000) 2483.
4. Alberto Varzi, Corina Täubert, Margret Wohlfahrt-Mehrens , Martin Kreis, and Walter Schütz, Study of multi-walled carbon nanotubes for lithium-ion battery electrodes, *Journal of Power Sources*, 196 (2011) 3303.
5. I. H. Kim and K. B. Kim, Ruthenium Oxide Thin Film Electrodes for Supercapacitors, *Electrochemical and Solid State Letters*, 4 (2001), A62
6. Rojas-Cessa, R., Grebel, H., Jiang, Z., Fukuda, C., Pita, H., Chowdhury, T. S., Dong, Z. and Wan, Y. FEW: Integration of alternative energy sources into digital micro-grids. *Environ. Prog. Sustainable Energy* (2017), *Environ. Prog. Sustainable Energy*. doi:10.1002/ep.12725
7. T. Selim Chowdhury and H. Grebel, Electrically tuned super-capacitors, <https://arxiv.org/pdf/1512.08000>
8. Haim Grebel and Yan Zhang, Controlling Ionic Currents with Transistor-like Structures, *ECS Trans.* 2 (2007), 1-18; doi: 10.1149/1.2408981
9. Sreeya Sreevatsa, Amrita Banerjee and Grebel Haim, Graphene as a Permeable Ionic Barrier, *ECS Trans.* 19 (2009) 259-264. doi: 10.1149/1.3119550.
10. S. Sreevatsa and H. Grebel, Carbon Nanotube Structures as Ionic Barriers: A New Corrosion Prevention Concept, *ECS #676 D1*, San Francisco, CA 2009. *ECS Trans.* 19 (2009) 91-100;

11. Amrita Banerjee and Haim Grebel, On the stopping potential of ionic currents, *Electrochem. Commun.* (2010), doi:10.1016/j.elecom.2009.12.013.
12. Joel Grebel, Amrita Banerjee and Haim Grebel, Towards bi-carrier ion-transistors: DC and optically induced effects in electrically controlled electrochemical cells, *Electrochimica Acta*, 95 (2013) 308–312.
13. T. Chowdhury and H. Grebel, Effect of Gate Electrode in Electrochemical Cells, Session B01: Energy Storage: Batteries and Supercapacitors, Abstract MA2015-01 721, 227 ECS Annual Meeting, Chicago, IL, (May 2015)
14. H. Grebel, Logic gates with ion transistors, *Thin Solid Films*, 638, (2017) 138-143
15. H. Grebel and P. Chen, Artificial dielectric polymeric waveguides: semiconductor-embedded films, *Opt. Lett.* 15 (1990) 667-669.
16. R. Collin, “Field Theory of Guided Waves”, Wiley-IEEE Press, ISBN: 978-0-87942-237-0.